https://doi.org/10.5194/essd-2019-174
Preprint. Discussion started: 23 January 2020

Open Access Earth System Science Data Discussions

Spatial radionuclide deposition data from the 60 km area around the Chernobyl nuclear power plant: results from a sampling survey in 1987.

Valery Kashparov[1,3], Sviatoslav Levchuk[1], Marina Zhurba[1], Valentyn Protsak[1], Nicholas A. Beresford[2], and Jacqueline S. Chaplow[2]

[1] Ukrainian Institute of Agricultural Radiology of National University of Life and Environmental Sciences of Ukraine, Mashinobudivnykiv str.7, Chabany, Kyiv region, 08162 Ukraine

[2] UK Centre for Ecology & Hydrology, Lancaster Environment Centre, Library Avenue, Bailrigg, Lancaster, LA1 4AP, UK

[3] CERAD CoE Environmental Radioactivity/Department of Environmental Sciences, Norwegian University of Life Sciences, 1432 Aas, Norway

Correspondence to: Jacqueline S. Chaplow (jgar@ceh.ac.uk)

Abstract. The dataset "Spatial radionuclide deposition data from the 60 km area around the Chernobyl nuclear power plant: results from a sampling survey in 1987" is the latest in a series of data to be published by the Environmental Information Data Centre (EIDC) describing samples collected and analysed following the Chernobyl nuclear power plant accident in 1986. The data result from a survey carried out by the Ukrainian Institute of Agricultural Radiology (UIAR) in April and May 1987 and include information on sample sites, dose rate, radionuclide (zirconium-95, niobium-95, ruthenium-106, caesium-134, caesium-137 and cerium-144) deposition, and exchangeable caesium-134 and 137.

The purpose of this paper is to describe the available data and methodology used to obtain them. The data will be useful in the reconstruction of doses to human and wildlife populations, answering the current lack of scientific consensus on the effects of radiation on wildlife in the Chernobyl Exclusion zone and in evaluating future management options for Chernobyl impacted area of Ukraine and Belarus.

The data and supporting documentation are freely available from the Environmental Information Data Centre (EIDC) under the terms and conditions of the Open Government Licence (Kashparov et al., 2019 https://doi.org/10.5285/a408ac9d-763e-4f4c-ba72-73bc2d1f596d).

1 Background

The dynamics of the releases of radioactive substance from the number four reactor at the Chernobyl nuclear power plant (ChNPP) and meteorological conditions (Chernobyl, 1996) over the ten days following the accident on the 26th April 1986 resulted in a complex pattern of contamination over a vast area (De Cort et al., 1998; IAEA, 2006).

The neutron flux rise and a sharp increase in energy emission at the time of the accident resulted in heating of the nuclear fuel and leakage of fission products. Destruction of the fuel rods caused an increase in heat transfer to the surface of the superheated fuel particles and coolant, and release of radioactive substances into the atmosphere (Kashparov et al., 1996). According to the latest estimates (Kashparov et al., 2003; UNSCEAR, 2008) 100% of inert radioactive gases (largely ^{85}Kr and ^{133}Xe), 20-60% of iodine isotopes, 12-40% of ^{134,137}Cs and 1.4-4% of less volatile radionuclides (^{95}Zr, ^{99}Mo, ^{89,90} Sr, ^{103,106} Ru, ^{141,144} Ce, ^{154,155} Eu, $^{238-241}$ Pu etc.) in the reactor at the moment of the accident were released to the atmosphere.

As a result of the initial explosion on 26th April 1986, a narrow (100 km long and up to 1 km wide) relatively straight trace of radioactive fallout formed to the west of the reactor in the direction of Red Forest and Tolsty Les village (this has subsequently become known as the 'western trace'). This trace was mainly finely dispersed nuclear fuel (Kashparov et al., 2003,

https://doi.org/10.5194/essd-2019-174
Preprint. Discussion started: 23 January 2020

2018) and could only have been formed as a consequence of the short-term release of fuel particles with overheated vapour to a comparatively low height during night time (the accident occurred at 01:24) stable atmospheric conditions. At the time of the accident, surface winds were weak and did not have any particular direction; only at a height of 1500 m was there a south-western wind with the velocity 8-10 $m \cdot s^{-1}$ (IAEA, 1992). Cooling of the release cloud, which included steam, resulted in the decrease of its volume, water condensation and wet deposition of radionuclides as mist (as the released steam cooled) (Saji, 2005). Later the main mechanism of fuel particle formation was the oxidation of the nuclear fuel (Kashparov et al., 1996; Salbu et al., 1994). There was an absence of data on meteorological conditions in the area of ChNPP at the time of the accident (the closest observations were for a distance of more than 100 km away to the west (Izrael et al., 1990)). There was also a lack of source term information and data on the composition of dispersed radioactive fallout. Consequently, it was not possible to make accurate predictions of deposition for the area close to the ChNPP (Talerko, 2005).

The relative leakage of fission products of uranium (IV) oxide in an inert environment at temperatures up to 2600 °C decreases in the order: volatile (Xe, Kr, I, Cs, Te, Sb, Ag), semi-volatile (Mo, Ba, Rh, Pd, Tc) and nonvolatile (Sr, Y, Nb, Ru, La, Ce, Eu) fission products (Kashparov et al., 1996; Pontillon et al., 2010). As a result of the estimated potential remaining heat release from fuel at the time of the accident (~230 W kg^{-1} U) and the heat accumulation in fuel (National Report of Ukraine, 2011), highly mobile volatile fission products (Kr, Xe, iodine, tellurium, caesium) were released from the fuel of the reactor and raised to a height of more than 1 km on 26th April 1986 and to *c*. 600 m over the following days (IAEA, 1992; Izrael et al., 1990). The greatest release of radiocesium occurred during the period of maximum heating of the reactor fuel on 26-28th April 1986 (Izrael et al., 1990). This caused the formation of the western, south-western (towards the settlements of Poliske and Bober), north-western (ultimately spreading to Sweden and wider areas of western Europe), and north-eastern condensed radioactive traces. Caesium deposition at distances from Chernobyl was largely determined by the degree of precipitation (e.g. see Chaplow et al. (2015) discussing deposition across Great Britain). After the covering of the reactor by dropping materials (including, 40 t of boron carbide, 2500 t of lead, 1800 t of sand and clay, 800 t of dolomite) from helicopters over the period 27th April–10th May 1986 (National Report of Ukraine. 2011), the ability for heat exchange of the fuel reduced, which caused a rise of temperature and consequent increase of the leakage of volatile fission products and the melting of the materials which had been dropped onto the reactor. Subsequently, there was a sharp reduction in the releases of radionuclides from the destroyed reactor on 6th May 1986 (National Report of Ukraine. 2011) due to aluminosilicates forming thermally stable compounds with many fission products and fixing caesium and strontium at high temperature (a process known prior to the Chernobyl accident (Hilpert & Nurberg, 1983)).

The changes of the annealing temperature of the nuclear fuel during the accident had a strong effect on both the ratio of different volatile fission products released (the migratory properties of Xe, Kr, I, Te, Cs increased with the temperature rise and were influenced by the presence of UO_2) and the rate of destruction of the nuclear fuel which oxidised forming micronized fuel particles (Salbu et al., 1994; Kashparov et al., 1996). The deposition of radionuclides such as ^{90}Sr, $^{238\text{-}241}Pu$, ^{241}Am, which were associated with the fuel component of the Chernobyl releases was largely limited to areas relatively close to the ChNPP. Areas receiving deposition of these

https://doi.org/10.5194/essd-2019-174
Preprint. Discussion started: 23 January 2020

radionuclides were the Chernobyl Exclusion Zone (i.e. the area of approximately 30 km radius around the ChNPP), and adjacent territories in the north of the Kiev region, in the west of the Chernihiv region, and the Bragin and Hoyniki districts of the Gomel region (Belarus). Deposition was related to the rate of the dry gravitational sedimentation of the fuel particles caused by their high density (about 8-10 g·cm^{-3} (Kashparov et al., 1996)); sedimentation of the lightweight condensation particles, containing iodine and caesium radioisotopes, was lower and hence these were transported further.

After the Chernobyl accident, western Europe and the Ukrainian-Belorussian Polessye were contaminated with radionuclides (IAEA, 1991, 1992, 2006). However, the area extending to 60-km around the ChNPP was the most contaminated (Izrael et al., 1990). Work on the assessment of the radiological situation within the zone started within a few days of the accident; the aim of this work was the radiation protection of the population and personnel.

Further quantification of terrestrial dose rates was carried out by aerial-gamma survey by the State Hydrometeorological Committee together with Ministry of Geology and Ministry of Defence of USSR (Izrael et al., 1990). Large-scale sampling of soil was also conducted, with samples analysed using gamma-spectrometry and radiochemistry methods (Izrael et al., 1990). The first results showed high variability in dose rates and radionuclide activity concentrations, with spatial patterns in both radioactive contamination and the radionuclide composition of fallout (Izrael et al., 1990).

The initial area from which the population was evacuated was based on an arbitrary decision whereby a circle around the Chernobyl nuclear power plant with a radius of 30 km was defined (IAEA, 1991). In the initial phase after the accident (before 7th May 1986) 99195 people were evacuated from 113 settlements including 11358 people from 51 villages in Belarus and 87 837 people from 62 settlements in Ukraine (including about 45 thousand people evacuated between 14.00-17.00 on April 27 from the town of Pripyat located 4 km from the ChNPP).

The analysis of data available in May 1986 showed that the extent of the territory with radioactive contamination where comprehensive measures were required to protect the population extended far beyond the 30-km Chernobyl Exclusion Zone (CEZ). A temporary annual effective dose limit of 100 mSv for the period from 26th April 1986 to 25th April 1987 (50 mSv from external and 50 mSv from internal exposure) was set by the USSR Ministry of Health. To identify areas outside of the CEZ where the population required evacuation, dose criteria had to be defined. It was proposed to use the average value of the dose rate of gamma radiation in open air for an area (estimated for 10th May, 1986) to help define an evacuation zone. An exposure dose rate of 5 mR h^{-1} estimated for 10th May 1986 (approximating to an effective dose rate (EDR) of gamma radiation in air of 50 μSv h^{-1}) equated to an external annual dose of 50 mSv for the period from 26th April 1986 to 25th April 1987.

At the end of May 1986 an approach to identifying areas where evacuation was required using estimated internal dose rates was proposed. This used the average density of the surface contamination of the soil with long-lived biologically significant nuclides (^{137}Cs, ^{90}Sr, ^{239,240}Pu) in a settlement and modelling to estimate the contamination of foodstuffs and hence diet. The numerical values suggested to identify areas for evacuation were: 15 Ci km^{-2} (555 kBq m^{-2}) of ^{137}Cs, 3 Ci km^{-2} (111 kBq m^{-2}) of ^{90}Sr and 0.1 Ci km^{-2} (3.7 kBq m^{-2}) of ^{239,240}Pu; this equated to an internal dose of 50 mSv over the first year after the accident.

https://doi.org/10.5194/essd-2019-174
Preprint. Discussion started: 23 January 2020

Open Access Earth System Science Data Discussions

However, in reality the main criterion for the evacuation was the exposure dose rate (R h^{-1}) and where the exposure dose rate exceeded 5 mR h^{-1} (EDR in air of about 50 μSv h^{-1}) the evacuated population were not allowed to return.

Hence, in 1986 the boundary of the population evacuation zone was set at an exposure dose rate of 5 mR h^{-1} (EDR of about 50 μSv h^{-1}). However, the ratio of short-lived gamma-emitting radionuclides (^{95}Zr, ^{95}Nb, ^{106}Ru, ^{144}Ce) deposited as fuel particles to ^{134,137}Cs deposited as condensation particles, was inconsistent across the evacuated areas. Therefore, after the radioactive decay of the short-lived radionuclides the residual dose rate across the evacuated areas varied considerably and was largely determined by the pattern of long-lived ^{137}Cs deposition (e.g. Figure 1) (Kashparov et al., 2018).

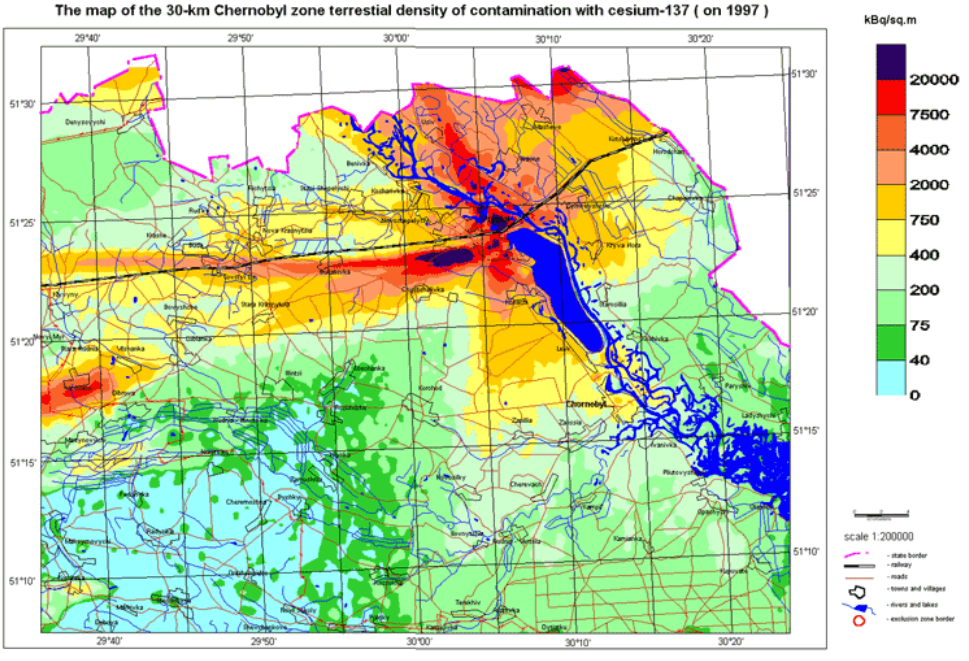

Figure 1. Caesium-137 deposition in the Ukrainian 30-km exclusion zone estimated for 1997 (from UIAR, 1998).

The first measurements of activity concentration of radionuclides in soil showed that radionuclide activity concentration ratios depended on distance and direction from the ChNPP (Izrael et al., 1990). Subsequent to this observation a detailed study of soil contamination was started in 1987 (Izrael et al., 1990). Taking into account the considerable heterogeneity of terrestrial contamination with radioactive substances in a large area, sampling along the western, southern and northern traces was carried out in stages finishing in 1988.

In 1987 the State Committee of Hydrometeorology of the USSR and the Scientific Centre of the Defence Ministry of the USSR established a survey programme to monitor radionuclide activity concentrations in soil. For this purpose, 540 sampling sites were identified at a distance

https://doi.org/10.5194/essd-2019-174
Preprint. Discussion started: 23 January 2020

Open Access Earth System Science Data Discussions

of 5 km to 60 km around the ChNPP using a polar coordinate system centred on the ChNPP. Fifteen sampling sites were selected on each of the 36 rays drawn every 10 degrees (Loshchilov et al., 1991) (Figure 3, 4). Radionuclide activity concentrations in 489 soil samples collected on the radial network were determined by the Ukrainian Institute of Agricultural Radiology (UIAR) and used to calculate the radionuclide contamination density. These data are discussed in this paper and the full dataset is freely available from Kashparov et al. (2019).

2 Data

The data (Kashparov et al., 2019) include location of sample sites (easting, northing, angle and distance from the ChNPP), dose rate, radionuclide deposition data, counting efficiency and information on exchangeable ^{134,137}Cs.

2.1 Sampling

To enable long-term monitoring and contamination mapping of the 60-km zone around the ChNPP 540 points were defined and sampled in April – May 1987. The sampling strategy used a radial network with points at every 10° (from 10° to 360°); sampling points were located at distances of 5 km, 6 km, 7 km, 8.3 km, 10 km, 12 km, 14.7 km, 17 km, 20 km, 25 km, 30 km, 37.5 km, 45 km, 52.5 km and 60 km (Figure 3, 4). The locations of sampling points were identified using maps and local landscape. Sites were resampled regularly until 1990 and sporadically thereafter, however, data for these subsequent samplings are not available (including to the UIAR).

Samples were not collected from points located in swamps, rivers and lakes; in total 489 samples were collected. A corer with a diameter of 14 cm was used to collect soil samples down to a depth of 5 cm from five points at each location using the envelope method (with approximately 5-10 m between sampling points) (Figure 2) (Loshchilov et al., 1991). Soil cores were retained intact during transportation to the laboratory. At each sampling point, the exposure dose rate was determined 1 m above ground level.

Figure 2. Soil sampling using a ring of 14 cm diameter to collect a 5 cm deep soil core (courtesy of UIAR, 1989).

https://doi.org/10.5194/essd-2019-174
Preprint. Discussion started: 23 January 2020

193
194 **2.2 Analysis**
195 Using a high-purity germanium detector (GEM-30185, ORTEC, USA) and a multichannel
196 analyser "ADCAM-300" (ORTEC, USA), the activity concentration of gamma emitting
197 radionuclides (^{95}Zr+^{95}Nd, ^{106}Ru, ^{134,137}Cs, ^{144}Ce) was determined in one soil sample from each
198 sampling site. Soil samples were analysed in a 1 litre Marinelli container. The other four cores
199 were sent to different laboratories in the Soviet Union (data for these cores are unfortunately
200 not available). Using a 1M NH_4Ac solution (pH 7) a 100 g subsample of soil was leached
201 (solid: liquid ratio 1:5). The resultant leachate solution was shaken for 1 hour and then left at
202 room temperature for 1 day before filtering through ashless filter paper (3-5 µm). The filtrate
203 was then put into a suitable container for gamma analysis to determine the fraction of
204 exchangeable ^{134,137}Cs. Measured activity concentrations were reported at 68% confidence
205 level (which equates to one standard deviation).
206
207 The density of soil contamination (Bq m^{-2}) was calculated from the estimated radionuclide
208 activity concentrations in soils. It has been estimated that using one soil sample (of area 0.015
209 m^2) is used to estimate a value of contamination density of the sampling site (i.e. the area from
210 which five cores were collected) the uncertainty may be up to 50% (Khomutinin et al., 2019).
211
212 The data described in this paper (Kashparov et al., 2019) comprise exposure dose rate (mR/h),
213 date of gamma activity measurement, density of contamination (Bq m^{-2}) of ^{95}Zr, ^{95}Nb, ^{106}Ru,
214 ^{134}Cs, ^{137}Cs and ^{144}Ce (with associated activity measurement uncertainties) and density of
215 contamination of $^{134+137}$Cs in exchangeable form. Reported radionuclide activity concentration
216 values are for the date of measurement (samples were analysed within 1.5 months of
217 collection).
218
219 **2.3 Results**
220
221 The contamination density of ^{144}Ce and ^{137}Cs are presented in Fig. 3 and 4; the activity
222 concentrations as presented in the figures have been decay corrected to 6th May 1986 the date
223 on which releases from the reactor in-effect stopped. The density of ^{144}Ce contamination
224 decreased exponentially with distance (Figures 3 and 5), because ^{144}Ce was released in the fuel
225 particles, which had a high dry deposition velocity (Kuriny et al., 1993). The fallout density of
226 ^{144}Ce decreased by 7-9 times between the 5 km and 30 km sampling sites, and by 70-120 times
227 between the 5 km and 60 km sampling sites (Figure 5).
228
229 The fallout density of ^{137}Cs decreased similarly to that of ^{144}Ce along the southern 'fuel trace'
230 (Figure 5a). The contamination density of ^{137}Cs along the western trace decreased less than the
231 ^{144}Ce contamination density due to the importance of the condensation component of the fallout
232 in this direction (Figure 5b). The comparative decrease of ^{137}Cs contamination density along
233 the northern trace (mixed fuel and condensation fallout) was in between that of the southern
234 and western traces (Figure 5c) although there were caesium hotspots in the northern
235 condensation trace (Figures 4 and 5c). The activity ratio of ^{144}Ce to ^{137}Cs decreased with
236 distance from the ChNPP due to the condensation component being more important for ^{137}Cs;
237 the condensation component had a lower deposition velocity compared with fuel particles (with
238 which ^{144}Ce was associated) (Figure 6). The ratio ^{144}Ce/^{137}Cs for Chernobyl reactor fuel on 6th
239 May 1986 can be estimated to be 15 from data presented in Table 1. The ratio was about 11
240 (geometric mean of 1167 measurements) in Chernobyl fuel particles larger than 10 µm due to
241 caesium escape during high-temperature annealing (Kuriny et al., 1993). The ratio of
242 ^{144}Ce/^{137}Cs in deposition exceeded five in the south-east and in the south up to 60 km and 30

https://doi.org/10.5194/essd-2019-174
Preprint. Discussion started: 23 January 2020

Open Access Earth System Science Data Discussions

km from the NPP respectively (Figure 6). Thus, activities of $^{134,137}Cs$ in the condensate and in the fuel components in these directions were of approximate equal importance. The condensation component of caesium was more important in the north and dominated in the west (Figure 8) (Loshchilov et al., 1991; Kuriny et al., 1993); the more rapidly changing $^{144}Ce/^{137}Cs$ ratios in these directions are reflective of this (Figure 6).

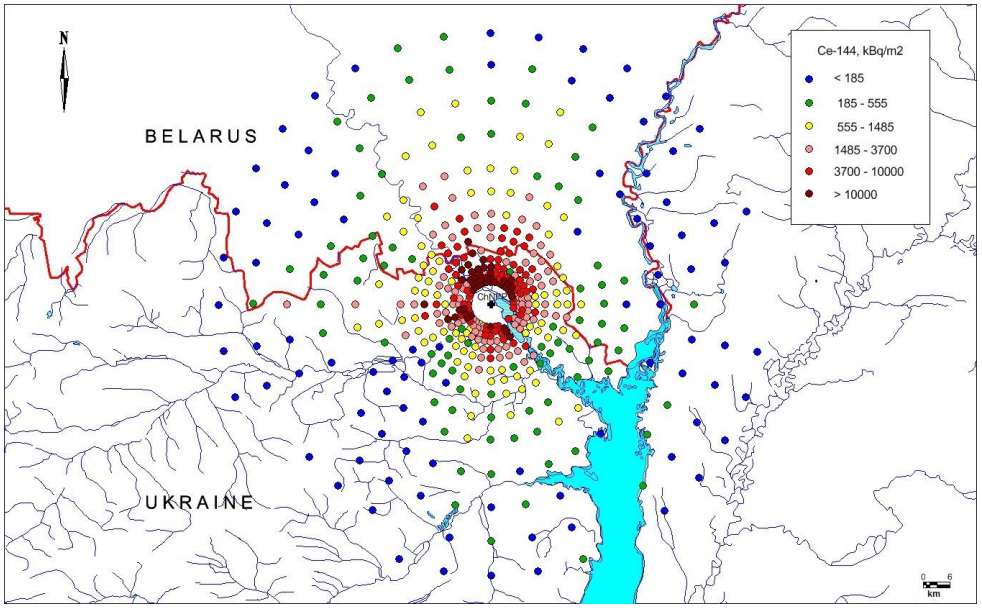

Figure 3. The fallout density of ^{144}Ce (kBq/m^2) within the 60 km zone around the ChNPP decay corrected to 6th May 1986.

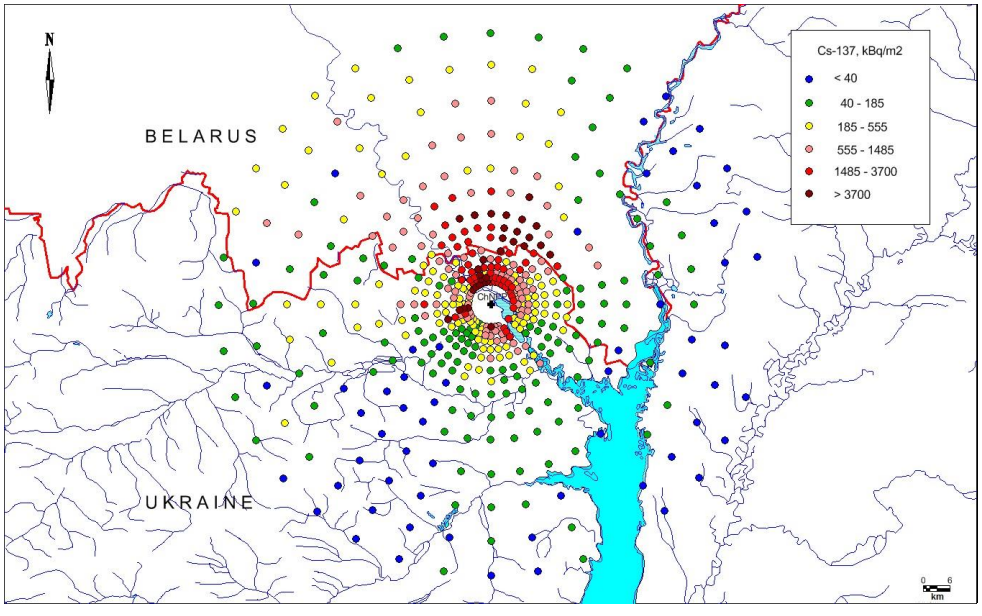

https://doi.org/10.5194/essd-2019-174
Preprint. Discussion started: 23 January 2020

Open Access Earth System Science Data Discussions

253 Figure 4. The fallout density of ^{137}Cs (kBq/m^2) within the 60 km zone around the ChNPP
254 decay corrected to 6th May 1986.

https://doi.org/10.5194/essd-2019-174
Preprint. Discussion started: 23 January 2020

Open Access Earth System Science Data Discussions

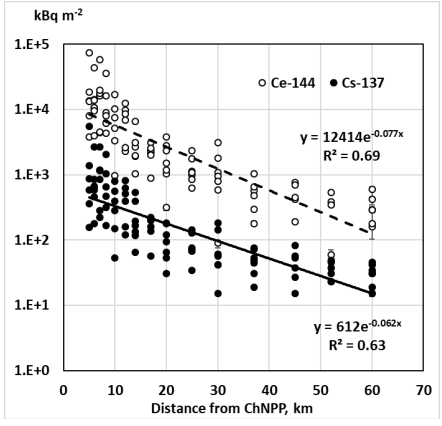

a

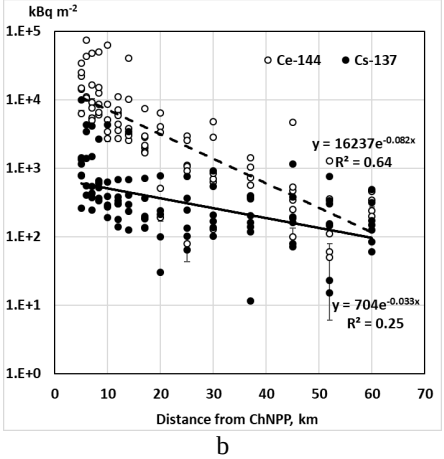

b

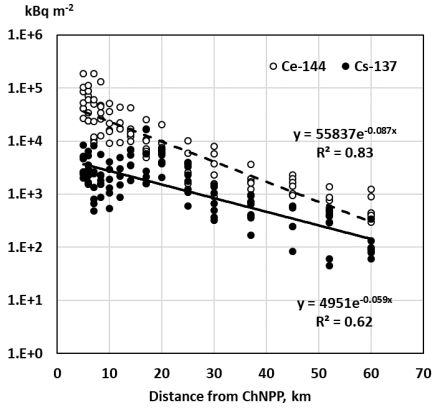

c

Figure 5. Relationship between fallout density of ^{144}Ce (1) and ^{137}Cs (2) and distance from the ChNPP towards the south (a) (150-210°), the west (b) (240-300°) and the north (c) (330-30°).

https://doi.org/10.5194/essd-2019-174
Preprint. Discussion started: 23 January 2020

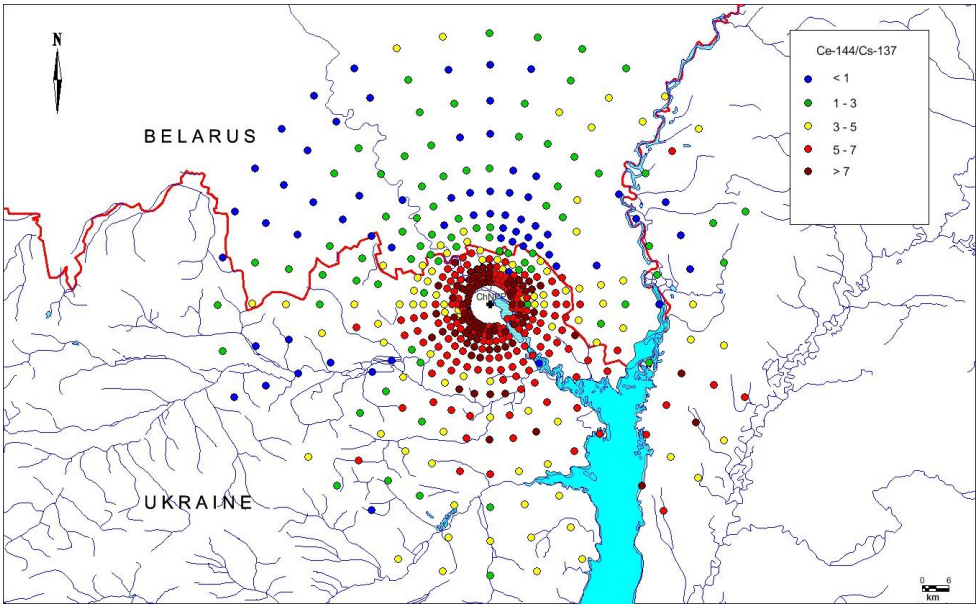

Figure 6. $^{144}Ce/^{137}Cs$ ratio within the 60 km zone around the ChNPP decay corrected to 6th May 1986.

Table 1. The average activity concentrations of radionuclides with half-life ($T_{1/2}$) >1 day estimated in the fuel of the ChNPP number four reactor recalculated for 6th May 1986 (Begichev et al., 1993).

Radionuclide	Half-life (days)	Average activity concentration (Bq g^{-1})	Radionuclide	Half-life (days)	Average activity concentration (Bq g^{-1})
^{75}Se	1.2E+02	5.40E+06	^{132}Te	3.3E+00	2.40E+10
^{76}As	1.1E+00	1.70E+07	^{133}Xe	5.2E+00	3.40E+10
^{77}As	1.6E+00	4.10E+07	^{134}Cs	7.6E+02	8.90E+08
^{82}Br	1.5E+00	1.80E+09	^{135}Cs	5.5E+07	1.90E+04
^{85}Kr	3.9E+03	1.50E+08	^{136}Cs	1.3E+01	3.30E+10
^{86}Rb	1.9E+01	8.70E+09	^{137}Cs	1.1E+04	1.40E+09
^{89}Sr	5.1E+01	2.10E+10	^{140}Ba	1.3E+01	3.20E+10
^{90}Sr	1.1E+04	1.20E+09	^{141}Ce	3.3E+01	2.90E+10
^{90}Y	1.1E+04	1.20E+09	^{143}Ce	1.4E+00	2.90E+10
^{91}Y	5.9E+01	2.60E+10	^{144}Ce	2.8E+02	2.10E+10
^{95}Zr	6.4E+01	3.10E+10	^{147}Nd	1.1E+01	1.10E+10
^{95}Nb	3.5E+01	3.00E+10	^{147}Pm	9.5E+02	4.20E+09
^{96}Nb	9.8E-01	3.10E+10	^{148m}Pm	4.1E+01	8.50E+09
^{99}Mo	2.7E+00	3.20E+10	^{149}Nd	2.2E+00	5.80E+09
^{99m}Tc	2.7E+00	2.80E+10	^{151}Pm	1.2E+00	2.60E+09

https://doi.org/10.5194/essd-2019-174
Preprint. Discussion started: 23 January 2020

^{103}Ru	3.9E+01	2.00E+10	^{151}Sm	3.3E+04	3.40E+07
^{105}Rh	1.5E+00	1.00E+10	^{153}Sm	1.9E+00	1.10E+09
^{106}Ru	3.7E+02	4.50E+09	^{154}Eu	3.1E+03	3.70E+07
^{110m}Ag	2.5E+02	5.30E+08	^{155}Eu	1.7E+03	4.85E+07
^{111}Ag	7.5E+00	4.40E+08	^{156}Eu	1.5E+01	1.90E+08
^{115m}In	1.9E-01	8.60E+07	^{160}Tb	7.2E+01	1.00E+07
^{117m} Sn	1.4E+01	8.30E+07	^{237}Np	7.8E+08	1.40E+03
^{123}Sn	1.3E+02	9.90E+07	^{239}Np	2.4E+00	3.10E+11
^{124}I	4.2E+00	1.40E+08	^{236}Pu	1.0E+03	6.00E+02
^{125}Sb	1.0E+03	7.80E+07	^{238}Pu	3.2E+04	6.80E+06
^{125m}Te	5.8E+01	1.60E+07	^{239}Pu	8.8E+06	5.00E+06
^{126m}Sb	1.2E+01	4.40E+08	^{240}Pu	2.4E+06	7.80E+06
^{126}Sb	1.2E+01	6.10E+07	^{241}Pu	5.1E+03	9.60E+08
^{127}Sb	3.8E+00	1.10E+09	^{242}Pu	1.4E+08	1.50E+04
^{127}Te	1.1E+02	8.90E+08	^{241}Am	1.6E+05	8.70E+05
^{129m}Te	3.3E+01	5.50E+09	^{243}Am	2.7E+06	5.10E+04
^{131}I	8.0E+00	1.60E+10	^{242}Cm	1.6E+02	2.30E+08
^{131m}Xe	1.2E+01	1.80E+08	^{244}Cm	6.6E+03	2.20E+06

A good correlation (R^2=0.98) was observed between fallout densities of ^{95}Zr (estimated from the activity concentration of daughter product ^{95}Nb)[1] and ^{144}Ce (Figure 7a) because both radionuclides were released and deposited as fuel particles (Kuriny et al., 1993; Kashparov et al., 2003; Kashparov, 2003). The fallout density ratio of ^{144}Ce/^{95}Zr=0.73±0.05, decay corrected to 6th May 1986, was similar to that estimated for Chernobyl reactor fuel (^{144}Ce/^{95}Zr=0.68) (Table 1).

The activity ratio of ^{144}Ce to ^{106}Ru in fallout was correlated (R^2=0.93) and was 3.9±0.4 decay corrected to 6th May 1986 (Figure 7b). The value was close to the ratio of ^{144}Ce/^{106}Ru estimated for fuel in the ChNPP number four reactor (4.7) (Table 1). Excess ^{106}Ru activity relative to ^{144}Ce activity in some soil samples was observed likely due to the presence of "ruthenium particles" (a matrix of iron group elements with a high content of ^{103,106}Ru (Kuriny et al., 1993; Kashparov et al., 1996)).

There was a weak correlation (R^2=0.41) between ^{144}Ce and ^{137}Cs activities in the fallout because, as already discussed, caesium was largely deposited as condensation particles while cerium was deposited in fuel particles only. However, in highly contaminated areas close to the ChNPP a significant part of the ^{137}Cs was deposited as fuel particles and the activity ratio of ^{144}Ce/^{137}Cs of 9.1 (Figure 7c) broadly corresponded to that of 15 in the reactor fuel (Table 1).

Different radioisotopes of caesium escaped from nuclear fuel and were deposited in the same way. This similar behaviour of ^{134}Cs and ^{137}Cs resulted in a strong correlation (R^2=0.99)

[1] Niobium-95 ($T_{1/2}$=34 days) is the daughter radionuclide of ^{95}Zr ($T_{1/2}$=65 days) and the ratio of their activities at an equilibrium equals ^{95}Nb/^{95}Zr=2.1.

https://doi.org/10.5194/essd-2019-174
Preprint. Discussion started: 23 January 2020

Open Access Earth System Science Data Discussions

between their activities in soil samples and the ratio of $^{134}Cs/^{137}Cs=0.57\pm0.07$ was similar to that estimated for the reactor fuel (0.64, Table 1).

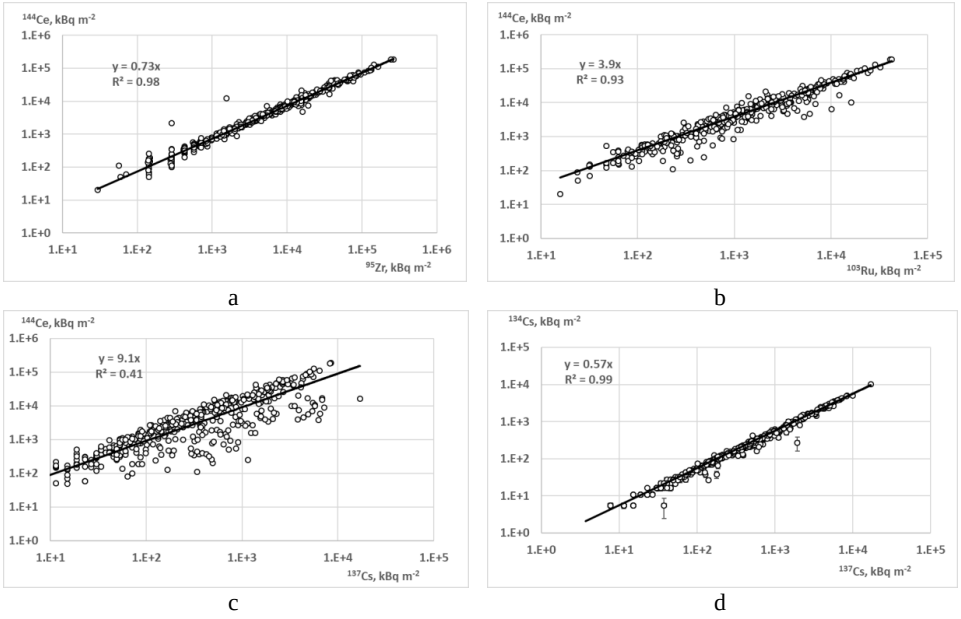

Figure 7. Correlation between deposition densities of different radionuclides decay corrected to 6th May 1986.

3 Use of the data

Apart from adding to the available data with which contamination maps for the CEZ and surrounding areas can be generated (e.g. Kashparov et al., 2018) the data discussed in this paper can be used to make predictions for less well studied radionuclides.

The determination of beta and alpha emitting radionuclides in samples requires radiochemical extraction which is both time consuming and relatively expensive. Large-scale surveys of the deposition of alpha and beta emitting radionuclides are therefore more difficult than those for gamma-emitting radionuclides and are not conducive with responding to a large-scale accident such as that which occurred at Chernobyl. Above we have demonstrated that the deposition behaviour of different groups of radionuclides was determined by the form in which they were present in the atmosphere (i.e. associated with fuel particles or condensation particles).

We propose that ^{144}Ce deposition can be used as a marker of the deposition of fuel particles; fuel particles were the main deposition form of nonvolatile radionuclides (i.e. Sr, Y, Nb, Ru, La, Ce, Eu, Np, Pu, Am, Cm). Therefore, using ^{144}Ce activity concentrations determined in soil samples and estimates of the activities in reactor fuel, we can make estimates of the deposition of radionuclides such as Pu-isotopes and Cm that have been relatively less studied. For example, activity ratios of ^{238}Pu, ^{239}Pu ^{240}Pu and ^{241}Pu to ^{144}Ce, at the time of measurement would be $8.4\times10^{-4,}$ 6.2×10^{-4}, 9.7×10^{-4} and 1.1×10^{-1} respectively (estimated by decay correcting data presented in Table 1). Fallout densities of these plutonium isotopes can therefore be

https://doi.org/10.5194/essd-2019-174
Preprint. Discussion started: 23 January 2020

Open Access Earth System Science Data Discussions

318 calculated for all sampling points where deposition density of ^{144}Ce was measured either in this
319 study (e.g. Figure 3) or in other datasets. As an example of the application of the data in this
320 manner, Fig. 8 presents the estimated deposition of ^{238}Pu. The first maps of ^{90}Sr and $^{239+240}$Pu
321 surface contamination from the Chernobyl accident were prepared in the frame of an
322 international project (IAEA, 1992) in a similar way.

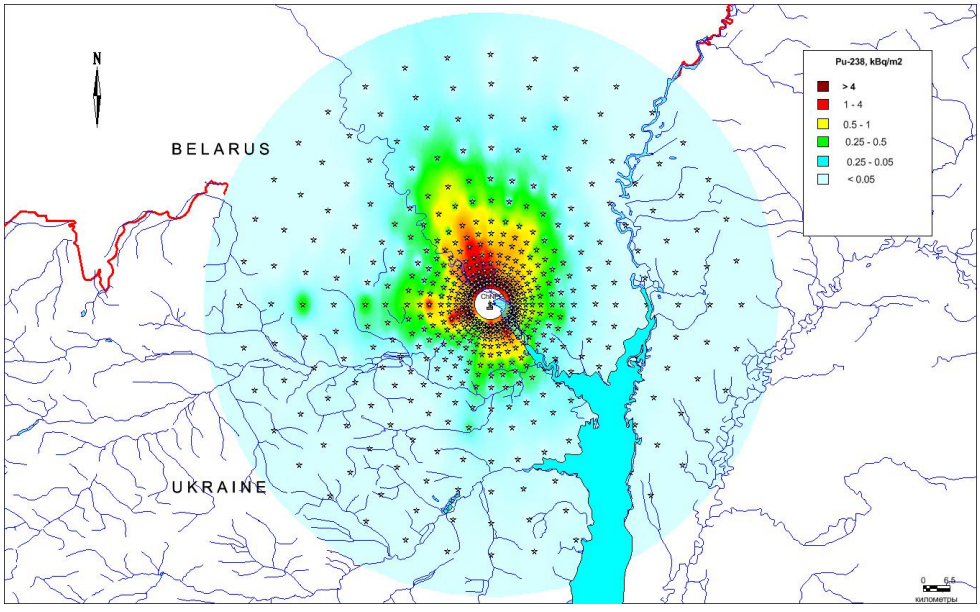

323

324

325 Figure 8. The fallout density of ^{238}Pu (kBq m^{-2}) corrected to 6th May 1986; estimated from
326 measurements of ^{144}Ce in soil and estimated activity concentrations in the fuel of the ChNNP
327 reactor number four.

328 The dynamic spatial distribution of gamma dose rate can be reconstructed using the data on
329 radionuclide contamination densities (Kashparov et al, 2019) in combination with the ratios
330 between activities of radionuclides in fuel and in condensed components of Chernobyl fallout
331 (Table 1) and also dose coefficients for exposure to contaminated ground surfaces, (Sv s^{-1}/Bq
332 m^{-2}) (Eckerman & Ryman, 1993). Five days after deposition the following radionuclides were
333 major contributors (about 95 %) to gamma dose rate: ^{136}Cs, ^{140}La, ^{239}Np, ^{95}Nb, ^{95}Zr, ^{131}I, ^{148m}
334 Pm, ^{103}Ru, ^{140}Ba, ^{132}Te. After three months the major external dose contributors were: ^{95}Nb,
335 ^{95}Zr, ^{148m}Pm, ^{134}Cs, ^{103}Ru, ^{137m}Ba, ^{110m}Ag, ^{136}Cs, ^{106}Rh. Three years after the major contributors
336 were ^{137m}Ba, ^{134}Cs, ^{106}Rh, ^{110m}Ag, ^{154}Eu. At the present time the gamma dose can be estimated
337 to be mainly (99%) due to the gamma-emitting daughter radionuclide of ^{137}Cs (^{137m}Ba). Bondar
338 (2015) from a survey of the CEZ along the Ukrainian-Belarussian border, showed a good
339 relationship between ^{137}Cs contamination ($A_{Cs\text{-}137}$, in the range of 17-7790 kBq m^{-2}) and
340 ambient dose rates at 1m above the ground (D_{ext}, in the range of 0.1-6.0 μSv h^{-1}). The
341 relationship was described by following equation with correlation coefficient of 0.99:

342 $$D_{ext} = 0.0009 \cdot A_{Cs\text{-}137} + 0.14.$$

https://doi.org/10.5194/essd-2019-174
Preprint. Discussion started: 23 January 2020

As an example of the application of the data in this manner, Fig. 9 presents the estimated external effective gamma dose rate five and 95 days after the cessation of the radioactive releases from the reactor on 6th May 1986.

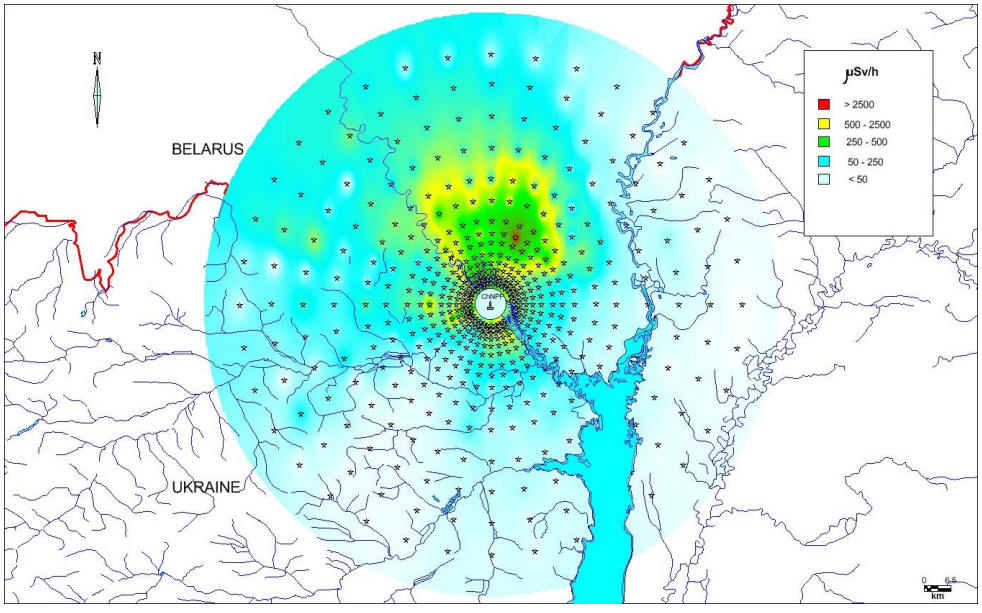

a

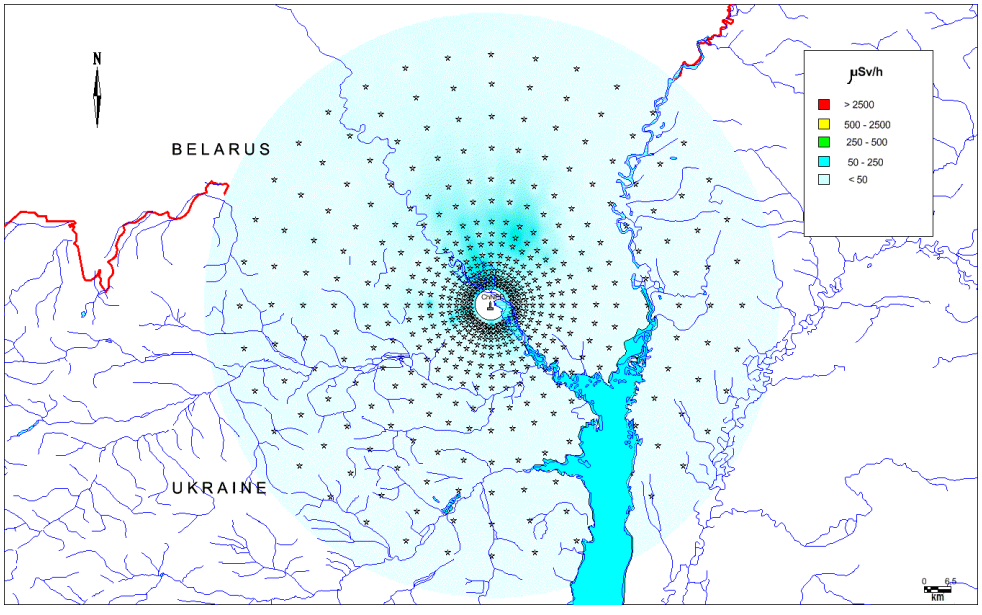

b

https://doi.org/10.5194/essd-2019-174
Preprint. Discussion started: 23 January 2020

Figure 9. Spatial distribution of effective dose rate within the 60km zone around the ChNPP on 10th May 1986 (a) and 10th August 1986 (b).

The estimated effective dose rate values exceed the evacuation dose criteria of 50 μSv h^{-1} over a large area (especially in the north and west) of the 60 km area around the ChNPP on 10th May 1986 (Figure 9a); as discussed above a dose rate of 50 μSv h^{-1} on 10th May 1986 equated to a total dose over the first year after the accident of 50 mSv - the value used to define areas for evacuation. On the 10th August 1986 the area estimated to exceed 50 μSv h^{-1} was restricted to the north (Figure 9b). The dose rate decreased quickly after the accident due to the radioactive decay of short-lived radionuclides. The dominance of these short-lived radionuclides and a lack of knowledge of the radionuclide composition of the fallout made it difficult in 1986 to estimate external dose rates to the public for an evaluation date of 10th May 1986 (most dose rate measurements being made after the 10th May). This likely resulted in the overestimation of dose rates for some villages in 1986 leading to their evacuation when the external dose rate would not have been in excess of the 50 mSv limit used by the authorities.

There is a need for deposition data for the CEZ and surrounding areas for a number of reasons. These include exploring risks associated with future management options for the CEZ (e.g. management of the water table, forest fire prevention, increased tourism, etc.) and also the return of abandoned areas outside of the CEZ to productive use. The long-term effect of radiation exposure on wildlife in the CEZ is an issue of much debate (e.g. see discussion in Beresford et al., 2019). Improved data which can be used to map the contamination of a range of radionuclides will be useful in improving dose assessments to wildlife (including retrospective assessments of earlier exposure rates). The CEZ has been declared a 'Radioecological Observatory' (Muikku et al., 2018) (where a Radioecology Observatory is defined as a radioactively contaminated field site that provides a focus for joint, long-term, radioecological research). The open provision of data as described in this paper fosters the spirit of collaboration and openness required to make the observatory site concept successful and joins a growing amount of data made available for the CEZ (Kashparov et al., 2017; Fuller et al., 2018; Kendrick et al., 2018; Gaschak et al., 2018; Beresford et al., 2018; Lerebours and Smith, 2019).

4 Data availability

The data described here have a digital object identifier (doi: 10.5285/a408ac9d-763e-4f4c-ba72-73bc2d1f596d) and are freely available for registered users from the NERC Environmental Information Data Centre (http://eidc.ceh.ac.uk/) under the terms of the Open Government Licence (Kashparov et al., 2019).

Competing interests. The authors declare that they have no conflict of interest.

Acknowledgements. Funding for UKCEH staff to contribute to preparing this paper and the accompanying dataset (Kashparov et al., 2019) was provided by the TREE (http://www.ceh.ac.uk/tree; funded by NERC, the Environment Agency and Radioactive Waste Management Ltd under the RATE programme) and associated iCLEAR (https://tree.ceh.ac.uk/content/iclear-0; funded by NERC) projects.

https://doi.org/10.5194/essd-2019-174
Preprint. Discussion started: 23 January 2020

References

Begichev S. N., Borovoy A.A., Burlakov E.V., Gavrilov S.L., Dovbenko A.A., Levina L.A., Markushev V.M., Marchenko A.E., Stroganov A.A., Tataurov A.L. Preprint IAE-5268/3: Reactor Fuel of Unit 4 of the Chernobyl NPP (a brief handbook). Kurchatov In st. Atomic Energy, 1990.

Beresford, N.A., Gaschak, S., Barnett, C.L., Maksimenko, A., Guliaichenko, E., Wells, C., Chaplow, J.S. A 'Reference Site' in the Chernobyl Exclusion Zone: radionuclide and stable element data, and estimated dose rates NERC-Environmental Information Data Centre. https://doi.org/10.5285/ae02f4e8-9486-4b47-93ef-e49dd9ddecd4, 2018.

Beresford, N.A., Scott, E.M., Copplestone, D. Field effects studies in the Chernobyl Exclusion Zone: Lessons to be learnt J. Environ. Radioact. https://doi.org/10.1016/j.jenvrad.2019.01.005, 2019

Bondar Yu. Field studies in the Chernobyl exclusion zone along the Belarusian border (dosimetric monitoring and soil radiation analysis). Report of Polesye State Radiation and Ecological Reserve. Belarus, Khoiniki, 2015.

Chaplow, J. S., Beresford, N. A., and Barnett, C. L.: Post-Chernobyl surveys of radiocaesium in soil, vegetation, wildlife and fungi in Great Britain, Earth Syst. Sci. Data, 7, 215–221, https://doi.org/10.5194/essd-7-215-2015, 2015.

Chernobyl Nuclear Power Plant and RBMK reactors.. Bulletin of Ecological Conditions of the Exclusion Zone 3: 4-8, 1996. (in Ukrainian, French).

De Cort, M., Dubois, G., Fridman, Sh. D., Germenchuk, M. G., Izrael, Yu. A., Janssens, A., Jones, A. R., Kelly, G. N., Kvasnikova, E. V., Matveenko, I., Nazarov, I. M., Pokumeiko, Yu. M., Sitak, V. A., Stukin, E. D., Tabachny, L. Ya., Tsaturov, Yu. S., and Avdyushin, S. I.: Atlas of caesium deposition on Europe after the Chernobyl accident, Luxembourg, Office for Official Publications of the European Communities, ISBN 92-828-3140-X, Catalogue YEAR?

Eckerman K.F. and Ryman J.C. External exposure to radionuclides in air, water, and soil. Federal guidance report No. 12, EPA-402-R-93-081, Oak Ridge National Laboratory, Tennessee 37831, USA, 238 P., 1993.

Fuller, N., Smith, J.T., Ford, A.T. Effects of low-dose ionising radiation on reproduction and DNA damage in marine and freshwater amphipod crustaceans. NERC Environmental Information Data Centre. https://doi.org/10.5285/b70afb8f-0a2b-40e6-aecc-ce484256bbfb, 2018.

Gaschak, S.P., Beresford, N.A., Barnett, C.L.; Wells, C., Maksimenko, A., Chaplow, J.S. 2018 Radionuclide data for vertebrates in the Chernobyl Exclusion Zone NERC-Environmental Information Data Centre. https://doi.org/10.5285/518f88df-bfe7-442e-97ad-922b5aef003a, 2018.

Hilpert K., Odoj R., and Nurnberg H. W.. Mass spectrometric study of the potential of Al203/Si02 additives for the retention of cesium in coated particles. Nucl. Technol., 61: 71, 1983.

IAEA. International Chernobyl Project: Technical Report. International Advisory Committee. Vienna, 1991.

IAEA. International Chernobyl project, technical report. ISBN 92-0-400192-5 (http://www-pub.iaea.org/MTCD/publications/PDF/Pub886_web/Start.pdf), 1992.

IAEA. Environmental consequences of the Chernobyl accident and their remediation: twenty years of experience. Report of the Chernobyl Forum Expert Group "Environment" (eds. L. Anspaugh and M. Balonov). Radiological assessment reports series, IAEA, STI/PUB/1239, 166 pp., 2006.

Izrael, Yu.A., Vakulovsky, S.M., Vetrov, V.A., Petrov, V.N., Rovinsky, F.Ya., Stukin, E.D.. Chernobyl: Radioactive Contamination of the Environment. Gidrometeoizdat publishers, Leningrad, 223 pp. 1990 (in Russian).

Kashparov, V. A.: Hot Particles at Chernobyl, Environ. Sci. Pollut. R., 10, 21–30, 2003.

Kashparov, V. A., Ivanov, Y. A., Zvarich, S. I., Protsak, V. P., Khomutinin, Y. V., Kurepin, A. D., and Pazukhin, E. M.: Formation of Hot Particles During the Chernobyl Nuclear Power Plant Accident, Nucl. Technol., 114, 246–253, 1996.

Kashparov, V.A.; Lundin, S.M.; Zvarich, S.I.; Yoschenko, V.I.; Levtchuk, S.E., Khomutinin, Yu.V., Maloshtan, I.N., Protsak, V.P. Territory contamination with the radionuclides representing the fuel component of Chernobyl fallout. The Science of the Total Environment. 317(1-3), 105-119. https://doi.org/10.1016/S0048-9697(03)00336-X, 2003.

Kashparov, V., Levchuk, S., Zhurba, M., Protsak, V., Khomutinin, Y., Beresford, N. A., and Chaplow, J. S.: Spatial datasets of radionuclide contamination in the Ukrainian Chernobyl Exclusion Zone, NERC-Environmental Information Data Centre, https://doi.org/10.5285/782ec845-2135-4698-8881-b38823e533bf, 2017.

https://doi.org/10.5194/essd-2019-174
Preprint. Discussion started: 23 January 2020

Kashparov, V.; Levchuk, S.; Zhurba, M.; Protsak, V.; Khomutinin, Yu.; Beresford, N.A.; Chaplow, J.S. Spatial datasets of radionuclide contamination in the Ukrainian Chernobyl Exclusion Zone. Earth System Science Data (ESSD). 10, 339-353. https://doi.org/10.5194/essd-10-339-2018, 2018.

Kashparov, V.; Levchuk, S.; Zhurba, M.; Protsak, V.; Beresford, N.A.; Chaplow, J.S. Spatial radionuclide deposition data from the 60 km radial area around the Chernobyl nuclear power plant, 1987. NERC Environmental Information Data Centre. https://doi.org/10.5285/a408ac9d-763e-4f4c-ba72-73bc2d1f596d, 2019.

Kendrick, P., Barçante, L., Beresford, N.A., Gashchak, S., Wood, M.D. Bird Vocalisation Activity (BiVA) database: annotated soundscapes from the Chernobyl Exclusion Zone. NERC Environmental Information Data Centre. https://doi.org/10.5285/be5639e9-75e9-4aa3-afdd-65ba80352591, 2018.

Khomutinin, Yu.; Fesenko, S.; Levchuk, S.; Zhebrovska, K.; Kashparov, V. Optimising sampling strategies for emergency response: 1. Soil. Journal of Environmental Radioactivity, 2019 (in press).

Kuriny, V. D., Ivanov, Y. A., Kashparov, V. A., Loschilov, N. A., Protsak, V. P., Yudin, E. B., Zhurba, M. A., and Parshakov, A. E.: Particle associated Chernobyl fall-out in the local and intermediate zones, Ann. Nucl. Energy, 20, 415–420, 1993.

Lerebours, A., Smith, J.T.. Water chemistry of seven lakes in Belarus and Ukraine 2014 to 2016. NERC Environmental Information Data Centre. https://doi.org/10.5285/b29d8ab8-9aa7-4f63-a03d-4ed176c32bf3, 2019.

Loshchilov, N. A., Kashparov, V. A., Yudin, Y. B., Protsak, V. P., Zhurba, M. A., and Parshakov, A. E.: Experimental assessment of radioactive fallout from the Chernobyl accident, Sicurezza e Protezione, 25–26, 46–49, 1991.

Muikku, M., Beresford, N.A., Garnier-Leplace, J., Real, A., Sirkka, L., Thorne, M., Vandenhove, H., Willrodt, C. Sustainability and integration of radioecology—position paper J. Radiol. Prot. 38, 152-163, http://iopscience.iop.org/article/10.1088/1361-6498/aa9c0b, 2018.

National Report of Ukraine. Twenty-five Years after Chornobyl Accident: Safety for the Future. – K.: KIM. – 328 p., 2011.

Pontillon, Y; Ducros, G; Malgouyres, P.P. 2010. Behaviour of fission products under severe PWR accident conditions VERCORS experimental programme—Part 1: General description of the programme. Nuclear Engineering and Design. 240(7), 1843–1852 https://doi.org/10.1016/j.nucengdes.2009.06.028, 2010.

Saji G. A scoping study on the environmental releases from the Chernobyl accident (part I): Fuel particles. American Nuclear Society International Topical Meeting on Probabilistic Safety Analysis, PSA 05: 685-696, 2005.

Salbu, B., Krekling, T., Oughton, D.H., Ostby, G., Kashparov, V.A., Brand, T.L., Day, J.P.. Hot Particles in Accidental Releases from Chernobyl and Windscale Nuclear Installations. Analyst 119: 125-130, 1994.

Talerko N.. Mesoscale modelling of radioactive contamination formation in Ukraine caused by the Chernobyl accident. J. of Env. Radioactivity. – 78: 311-329, 2005

UIAR: The map of the 30-km Chernobyl zone terrestrial density of contamination with cesium-137 (in 1997), UIAR, Kyiv, Ukraine, 1998.

United Nations Scientific Committee on the Effects of Atomic Radiation, UNSCEAR, Sources and effects of ionizing radiation. Report to the General Assembly with Scientific Annexes, volume II, Annex D. Health effects due to radiation from the Chernobyl accident. United Nations, New York, 178 pp., 2008.